THE ANNALS OF "DUNAREA DE JOS" UNIVERSITY OF GALATI
FASCICLE IX. METALLURGY AND MATERIALS SCIENCE
N°. 2 - 2025, ISSN 2668-4748; e-ISSN 2668-4756
Article DOI: https://doi.org/10.35219/mms.2025.2.03

ASSESSMENT USING NUMERICAL ANALYSIS OF THE BEHAVIOUR OF A TWO FINGERS GRIPPING MECHANISM

Ionuț LAMBRESCU, Mihai Bogdan-ROTH
Universitatea Petrol-Gaze din Ploieşti, Bd. Bucureşti 39, Ploieşti, Romania
e-mail: ilambrescu@upg-ploieşti.ro

ABSTRACT

An important issue in robotics is evaluating the force necessary to firmly grip objects. This can be done experimentally, or, as a more cost-effective approach, through numerical analysis. The results obtained through this method, although less precise, can offer a good assessment of the way a gripping mechanism behaves. The authors propose a comparative numerical analysis of a two-finger gripper, using a motion analysis performed in Siemens NX and a transient structural analysis conducted in Ansys. Both methods aim to capture the moment when the grasped object starts to slip. This moment marks the point at which the gripping is no longer reliable and provides insights into the reliability of the gripping mechanism. To assess the influence of the geometry of the gripping area, as well as the impact of the shape of the grasped object or the pair of materials (object and gripper), several analyses were performed in both Siemens NX and Ansys Workbench.

KEYWORDS: Gripping mechanisms, Grippers, Finite element, Motion analysis

1. Introduction

The problem of calculating/evaluating the force necessary for a firm grasp is of paramount importance in robotics. The literature covers this topic for a wide variety of grippers, in terms of their shape, number, material, etc. Some researchers analysed a static problem, while others considered the situation when the gripped object is moving (with a certain velocity or acceleration) [1, 2]. The proposed approaches were analytical, experimental, or numerical (or a combination of them). From the point of view of the shape of the grasped object, irregularly shaped objects are encountered in many cases [3-8].

The authors of this paper focused their research in two directions:

- To evaluate the friction coefficient for three pairs of materials: aluminium-aluminium, aluminium - Necuron and Necuron-Necuron;
- To include the determined friction coefficient in the analysis of a two-finger gripper (with different geometries in the grasping region – see Figure 1) used for grasping bodies of parallelepipedal, cylindrical, hyperboloidal, and barrel-like shapes (see Figure 2).

The analyses performed were done using (for comparison and validation) a motion analysis conducted in Siemens NX and a transient structural analysis carried out in Ansys Workbench. The main purpose of the analysis was to evaluate the influence of the grasped object shape and the geometry of the fingers' grasping area on the force necessary to retain the grasped object. Like other researchers [2, 9], we were interested in capturing the moment when the grasped object starts to slip. These moments in time, for various shapes of the grasped object and geometries of the fingers' contact areas, were compared to detect the influence they have on the stability of the grip.

The results will be presented in graphical format to allow the assessment of the influence that the object shape and the finger grasping region geometry have on the moment of inception of the slipping process.

THE ANNALS OF "DUNAREA DE JOS" UNIVERSITY OF GALATI
FASCICLE IX. METALLURGY AND MATERIALS SCIENCE
N°. 2 - 2025, ISSN 2668-4748; e-ISSN 2668-4756
Article DOI: https://doi.org/10.35219/mms.2025.2.03

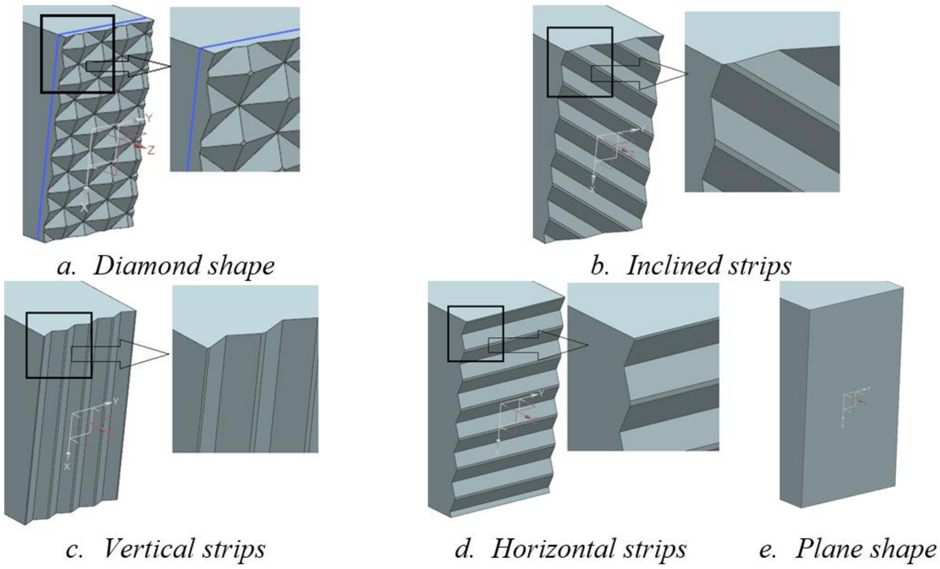

Fig. 1. *Geometries of the grasping region*

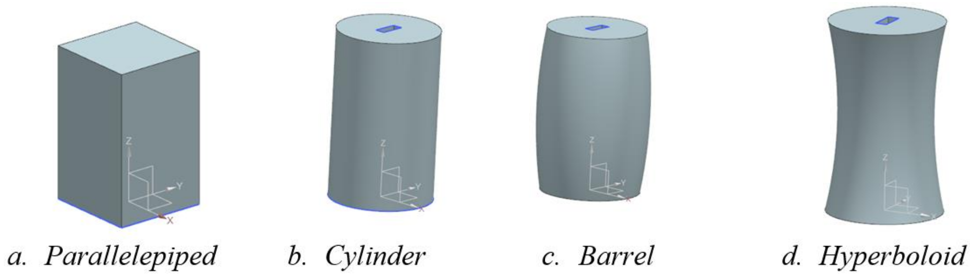

Fig. 2. *Shapes of the grasped objects*

2. Method

The workflow the authors propose is the following:

- Experimental determination of the friction coefficient for three material pairs: aluminum-aluminum, aluminum – Necuron (Necuron is a polymeric material with good performance in bending, compression and abrasion. It is used for tools, sheet metal forming, moulds for plastic deformation of metals, and prototypes for copying, etc. It can be glued with K8 and K13 adhesives. All the above-mentioned properties make Necuron a material worth considering for applications in robotics), and Necuron-Necuron;
- Capturing the moment of inception of slipping of the grasped object using a motion simulation in Siemens NX;
- Capturing the moment of inception of slipping of the grasped object using a transient structural analysis in Ansys Workbench (for the aluminum – aluminum pair only);
- Comparing and interpretation of the results.

Figure 3 provides details on the model used in the numerical analysis (motion simulation in Siemens NX).

The two fingers are pushed towards the object (they are in contact from the beginning) with forces acting along the two arrows, and with intensity described by the plot: the force remains constant for 0.2 seconds, then decays to zero over the next 0.8 seconds. The object rests on a moving base that executes a translation, as indicated by the arrow, at a speed of 200 mm/sec. After 0.2 seconds, the object is no longer supported by the moving base. As long as the two normal forces are sufficiently large, the object remains stationary. It will begin to slip when the normal forces no longer provide a frictional force capable of supporting the object's weight. This critical moment will be identified through numerical analysis.

THE ANNALS OF "DUNAREA DE JOS" UNIVERSITY OF GALATI
FASCICLE IX. METALLURGY AND MATERIALS SCIENCE
N°. 2 - 2025, ISSN 2668-4748; e-ISSN 2668-4756
Article DOI: https://doi.org/10.35219/mms.2025.2.03

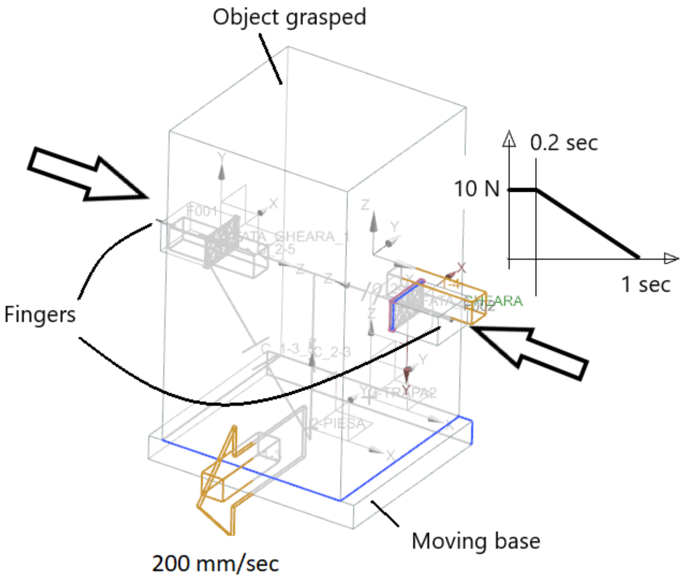

***Fig. 3.** The model for the analysis*

3. Determination of the friction coefficient

There are different methods presented in the literature for the experimental determination of the friction coefficient. We refer here to the contributions of [10-13]. The authors designed and built an original device for determining the friction coefficient for different pairs of materials – see Figure 4.

Basically, a normal force is applied to parts 1 and 2, which are in contact with the weighted object (part 5). The friction force holds this object in place if the normal forces have the required value. The applied force is continuously measured using the precision scale (part 3). The value of the normal force is controlled by the adjustment screw (part 4). When the normal force falls below a certain threshold, object 5 starts to slip.

Each determination is filmed. After each test, the AVI file is analysed using software that detects the moment the object begins to slip (move), and the corresponding normal force value is read from the display of the precision scale. Since the weight of object 5 and the normal force are known, it is straightforward to calculate the friction coefficient.

To assure reliable results, 201 determinations were carried out and statistically processed. After performing the Kolmogorov-Smirnov and the Shapiro-Wilk tests [14], which confirmed the normal distribution of the data, a mean value for the friction coefficient was calculated – see Figures 5a and 5b. After a simple calculation, the resulting friction coefficients for the three analysed material pairs were:

- aluminium-aluminium: 0.305;
- aluminium-Necuron: 0.318;
- Necuron-Necuron: 0.39.

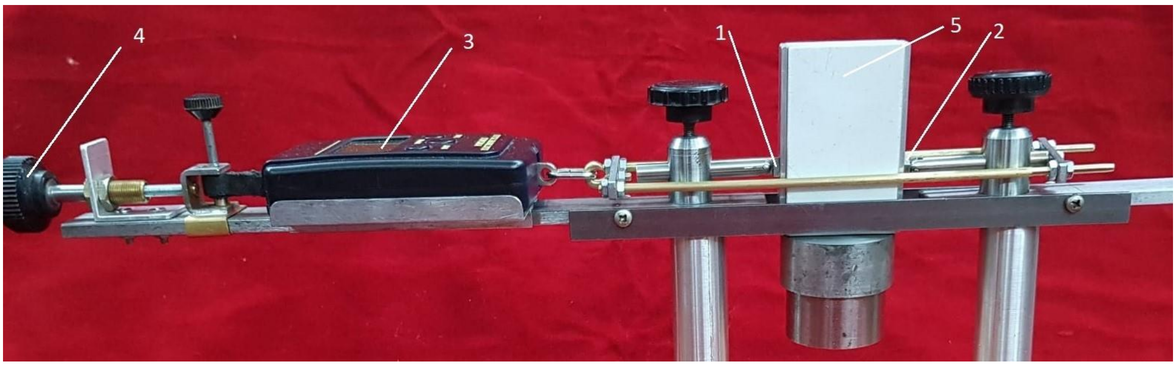

***Fig. 4.** Device for measuring the friction coefficient*

N°. 2 - 2025, ISSN 2668-4748; e-ISSN 2668-4756
Article DOI: https://doi.org/10.35219/mms.2025.2.03

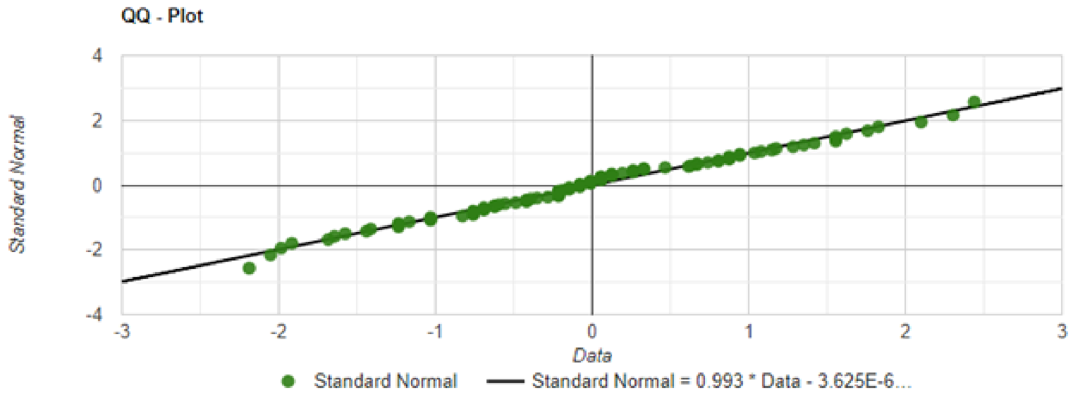

a) Standard Normal Distribution

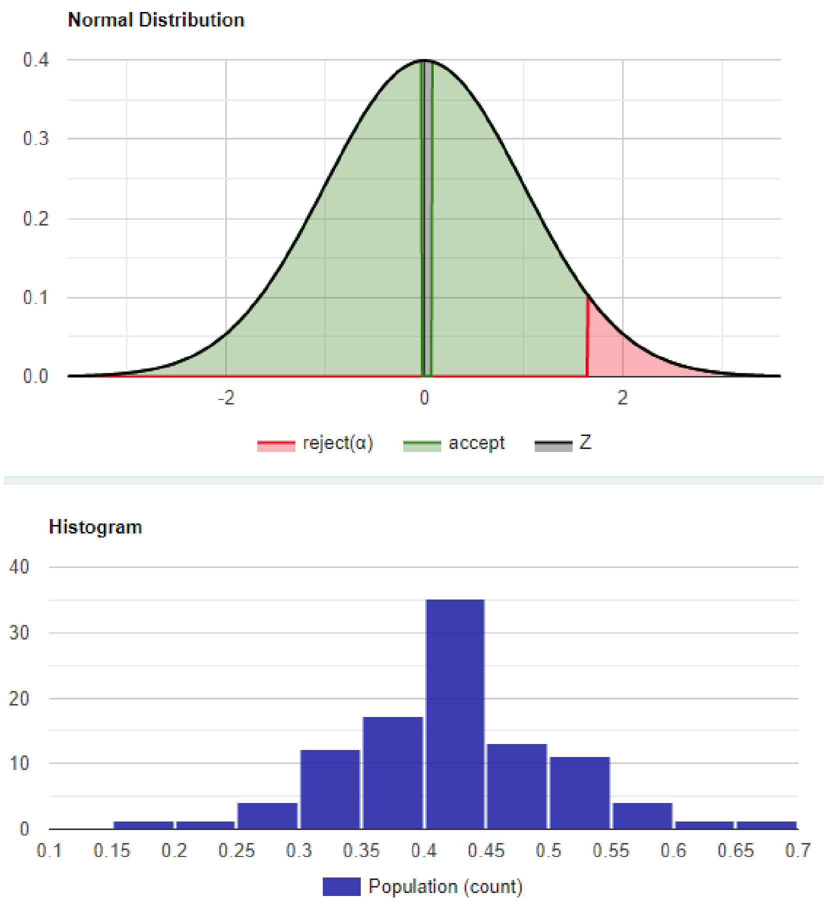

b) Normal distribution

Fig. 5. *Results of the Shapiro-Wilk test*

4. Dynamic analysis in Siemens NX

Figure 6 presents the model used in the Siemens NX dynamic simulation [15, 16]. Frame 1 is fixed. The Motion Base (part 3), as explained in the Method section and shown in Figure 3, moves and, after 0.2 seconds, leaves Object 2 with no support other than the friction forces acting between Object 2 and Fingers 4 and 5. When the normal forces applied through Fingers 4 and 5 on Object 2 become sufficiently small, Object 2 will begin to slip. Joints and 3D contacts were also defined in the simulation, and their names in the simulation tree indicate the bodies they connect - see Figure 6. The simulation was run for a duration of 1 second, with 200 equally spaced time steps.

N°. 2 - 2025, ISSN 2668-4748; e-ISSN 2668-4756
Article DOI: https://doi.org/10.35219/mms.2025.2.03

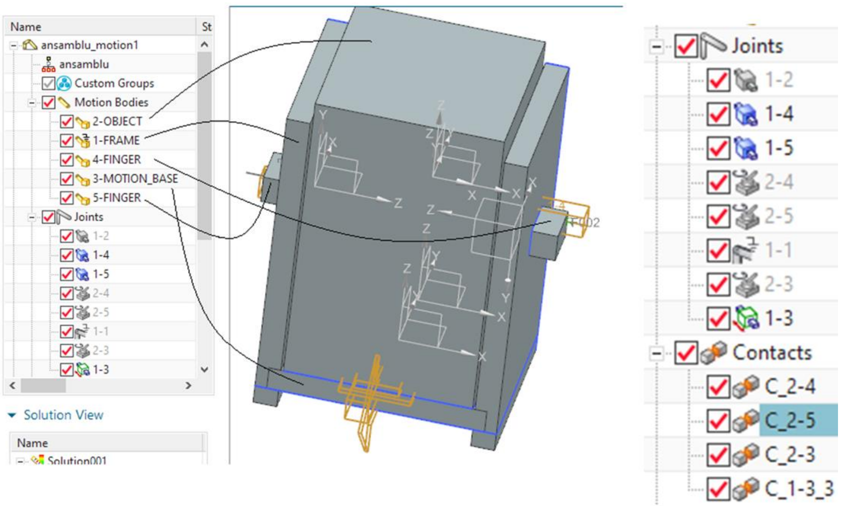

Fig. 6. *Model for the Siemens NX dynamic simulation*

After the analyses were performed for the different object shapes and finger geometries, results such as displacements, velocities, accelerations, and forces were obtained. These will be presented and discussed in Results and Conclusions sections.

5. Transient structural analysis in Ansys Workbench

Figure 7 presents the model used in the Ansys Workbench transient structural analysis [17]. The model is simpler than that used in the dynamic analysis performed in Siemens NX Motion. It includes one half of the Object and a Finger, with symmetry applied. This approach ensures a significant reduction in the number of elements.

Frictional contact has been defined between the half-Object and the Finger. Surface guides have also been defined for both components to ensure accurate replication of real-world boundary conditions. A force with a variation similar to that used in the Siemens NX motion analysis is applied to the Finger to produce friction between the Object and the Finger. After the analysis, results including displacements, velocities, accelerations, stress distributions, and contact conditions were obtained. These will be presented and discussed in Results and Conclusions sections.

The main settings of the transient structural analysis are as follows:

- Minimum time step: 0.001 seconds;
- Moderate speed dynamic;
- Large deflections: ON.

The minimum element size in the finger grasping area is 0.125 mm.

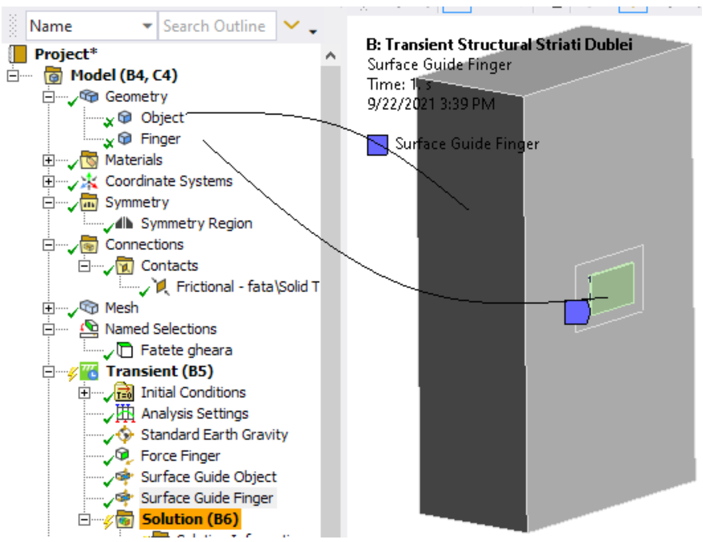

Fig. 7. *Model for the Ansys Workbench transient structural simulation*

THE ANNALS OF “DUNAREA DE JOS” UNIVERSITY OF GALATI
FASCICLE IX. METALLURGY AND MATERIALS SCIENCE
N°. 2 - 2025, ISSN 2668-4748; e-ISSN 2668-4756
Article DOI: https://doi.org/10.35219/mms.2025.2.03

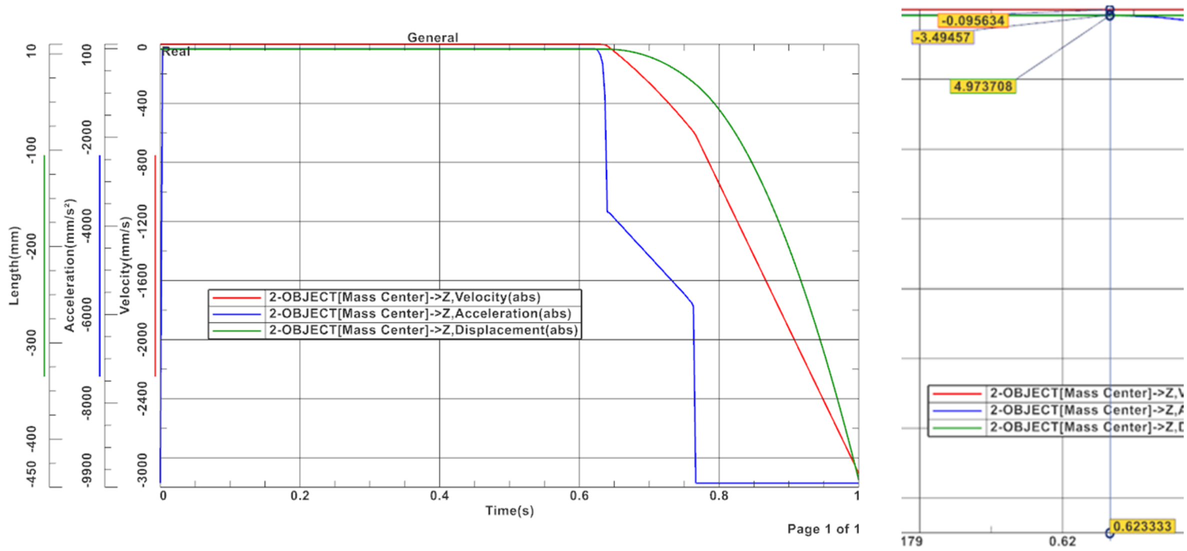

a) Overall view *b) Detail view*

Fig. 8. *Displacement [mm], velocity [mm/sec], acceleration [mm/sec^2] in the vertical direction*

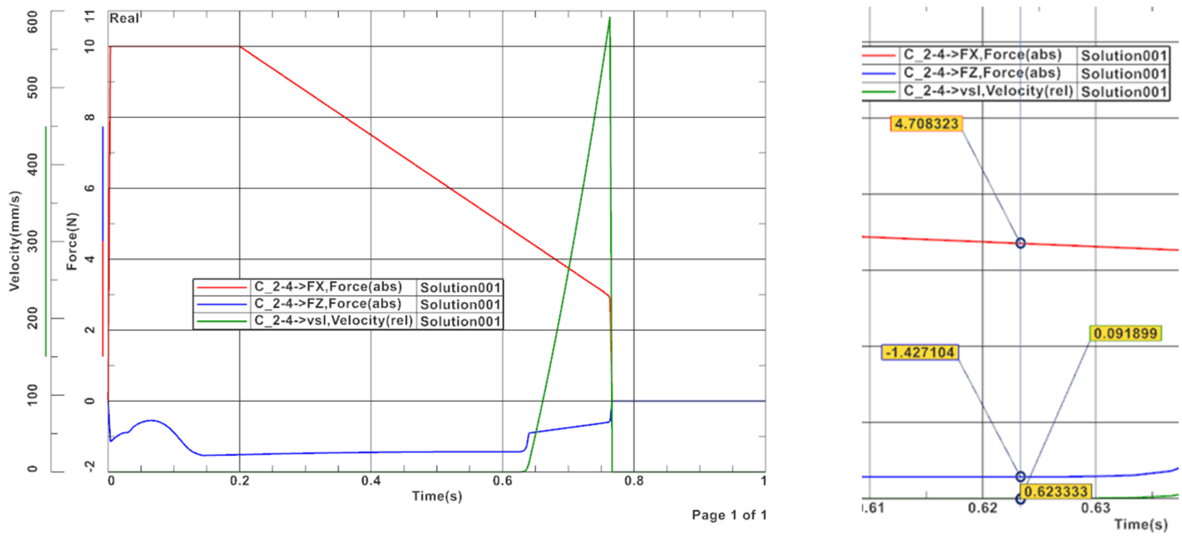

a) Overall view *b) Detail view*

Fig. 9. *Normal force (Fx), Friction force (Fz) [N] and Sliding velocity [mm/sec^2]*

As in the case of the motion analysis, using these plots and the accompanying tables, we can detect the moment when the object begins to slip. In the case of the data presented in Figures 10 and 11, we can observe that slipping starts at 0.625 seconds, which is very close to the moment detected in the Siemens NX motion analysis (0.623 seconds).

In the following plots, we will present the results obtained for all object shapes, finger geometries (in the grasping area), and material pairs, based on the motion analysis performed in Siemens NX. It is important to note that, regardless of the Object’s shape, the mass (weight) is kept strictly the same for all Objects.

Figures 12, 13, 14, and 15 aim to capture the influence of the material pair on the moment when the Object starts to slip.

Figures 16, 17, and 18 aim to capture the influence of the gripping area geometry on the moment the Object starts to slip.

THE ANNALS OF "DUNAREA DE JOS" UNIVERSITY OF GALATI
FASCICLE IX. METALLURGY AND MATERIALS SCIENCE
N°. 2 - 2025, ISSN 2668-4748; e-ISSN 2668-4756
Article DOI: https://doi.org/10.35219/mms.2025.2.03

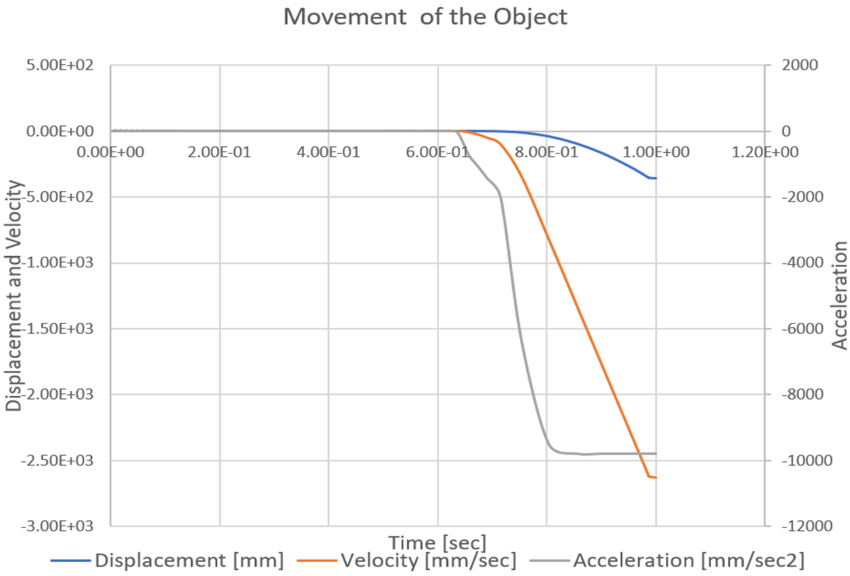

Fig. 10. *Displacement, Velocity and Acceleration for the Object*

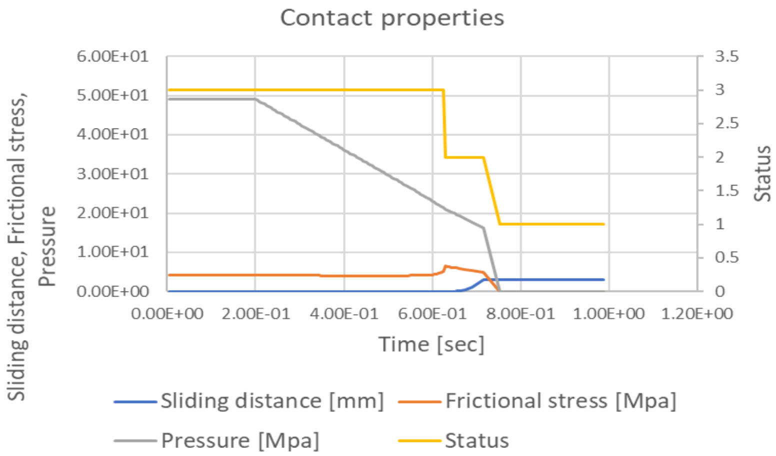

Fig. 11. *Contact properties*

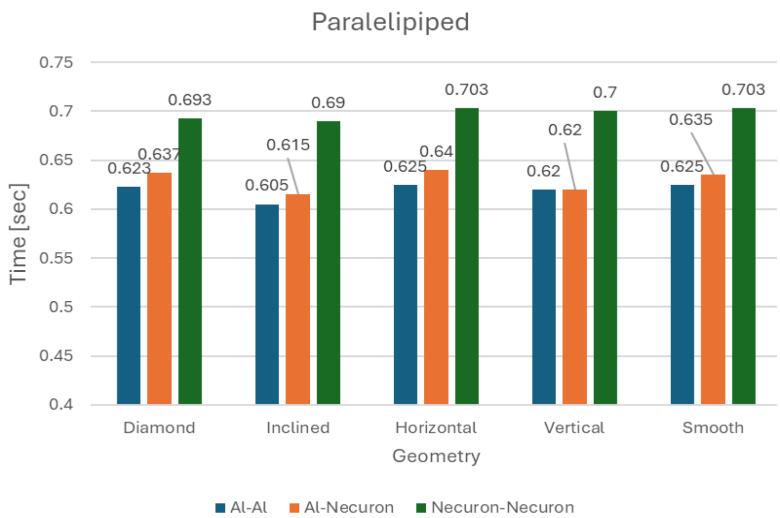

Fig. 12. *Moments in time when sliding initiates for the parallelepipedal Object*

THE ANNALS OF "DUNAREA DE JOS" UNIVERSITY OF GALATI
FASCICLE IX. METALLURGY AND MATERIALS SCIENCE
Nº. 2 - 2025, ISSN 2668-4748; e-ISSN 2668-4756
Article DOI: https://doi.org/10.35219/mms.2025.2.03

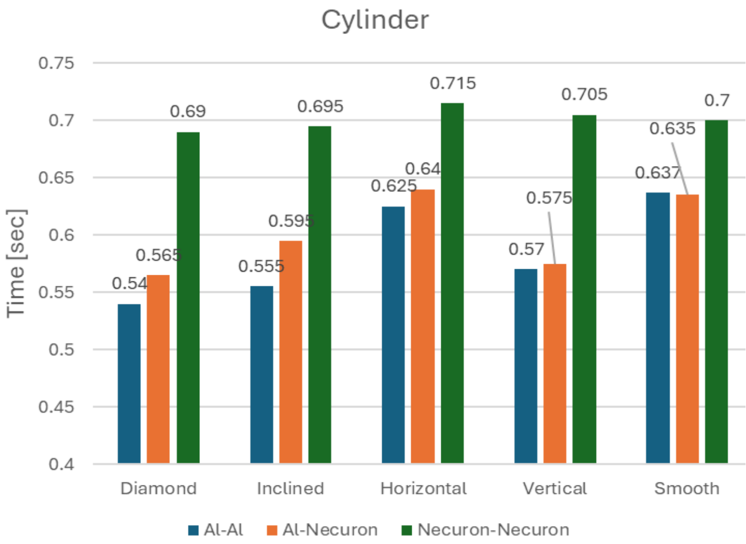

Fig. 13. *Moments in time when sliding initiates for the cylindrical Object*

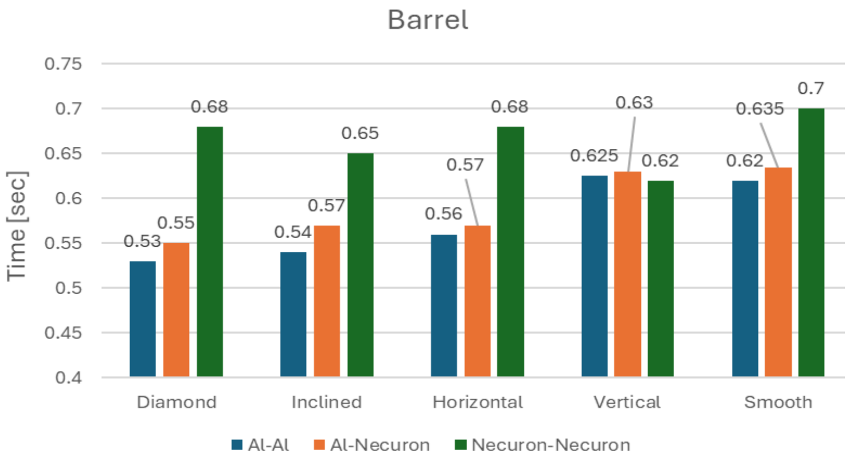

Fig. 14. *Moments in time when sliding initiates for the barrel Object*

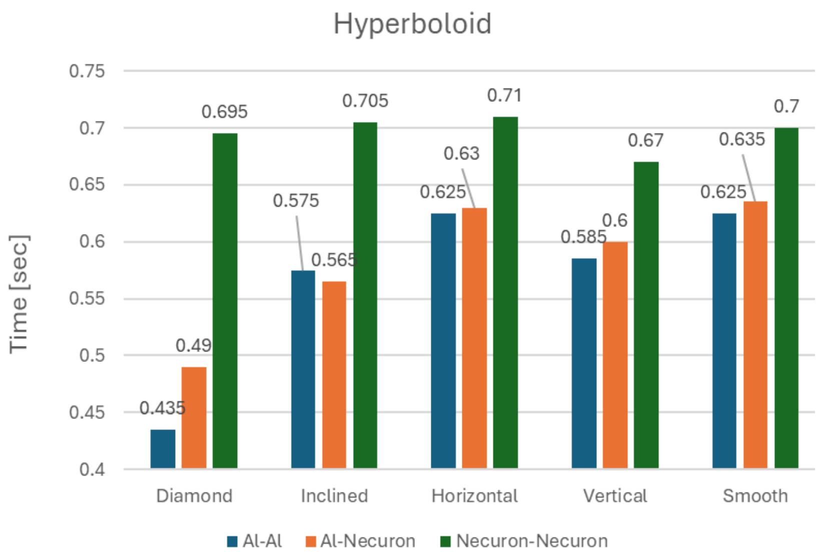

Fig. 15. *Moments in time when sliding initiates for the hyperboloidal Object*

Nº. 2 - 2025, ISSN 2668-4748; e-ISSN 2668-4756
Article DOI: https://doi.org/10.35219/mms.2025.2.03

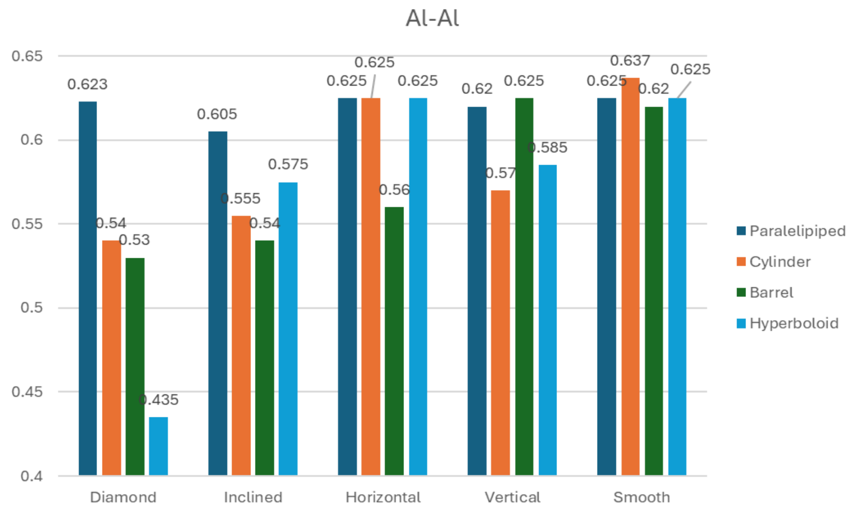

Fig. 16. Moments in time when sliding initiates for the Al-Al pair of materials

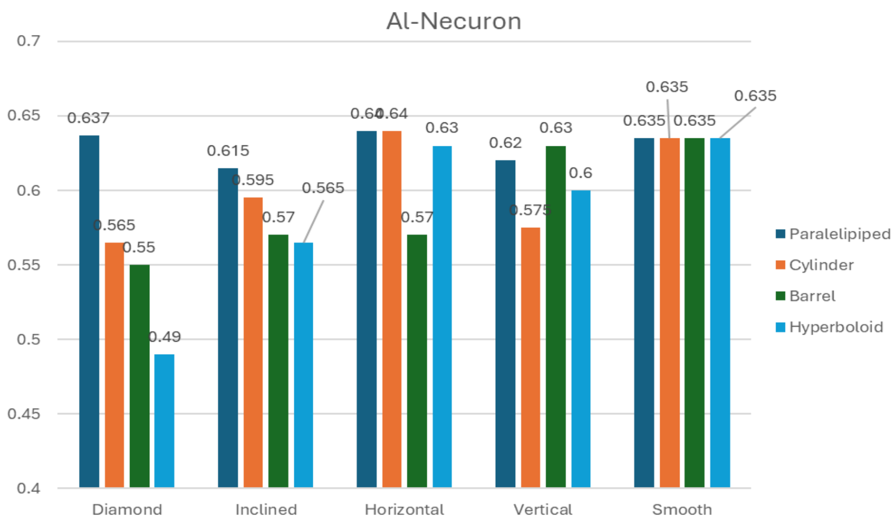

Fig. 17. Moments in time when sliding initiates for the Al-Necuron pair of materials

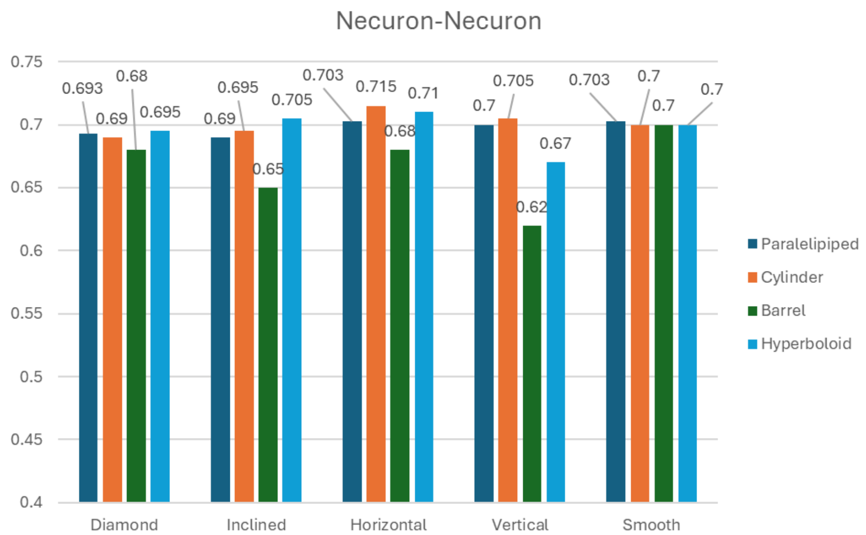

Fig. 18. Moments in time when sliding initiates for the Necuron-Necuron pair of materials

THE ANNALS OF "DUNAREA DE JOS" UNIVERSITY OF GALATI
FASCICLE IX. METALLURGY AND MATERIALS SCIENCE
N°. 2 - 2025, ISSN 2668-4748; e-ISSN 2668-4756
Article DOI: https://doi.org/10.35219/mms.2025.2.03

7. Discussions and Conclusions

All the bar plots present on the vertical axis moments in time (expressed in seconds) when the grip is lost, and the Object starts to move. Greater values of time mean lower values for the gripping force necessary to keep the Object in a still position.

Keeping this in mind, we can make the following remarks on the influence of the pair of materials on the stability of the gripping:

- For all shapes of the Object (Figures 12-15), the best pair of materials (requiring less gripping force) is Necuron-Necuron;
- If we want to assess the relative differences between the values over time, we can see in Table 1, that while in the case of Necuron-Necuron versus Al-Al or Necuron-Necuron versus Al-Necuron the differences cover the range of 10%-49%, with the largest differences seen for the hyperboloid-shaped Object, in the case of Al-Al and Al-Necuron the values are significantly smaller (with a maximal value of 12 % in the case of the hyperboloidal-shaped Object);
- In all cases, the "worst" pair of materials is Al-Al.

Figures 16, 17 and 18 allow us to better compare, graphically, the influence that the shape of the Object, along with the geometry in the gripping area, have on the efficiency of the grip. We can therefore make the following remarks:

Table 1. *Relative errors (for sliding velocity)*

		1	2	3			
		Sliding velocity			**Relative error [%]**		
		Al-Al	**Al-Nec**	**Nec-Nec**	**(3-1)/1**	**(3-2)/2**	**(2-1)/1**
Parallelepiped	Diamond	0.623	0.637	0.693	11.2%	8.8%	2.2%
	Inclined	0.605	0.615	0.69	14.0%	12.2%	1.7%
	Horizontal	0.625	0.64	0.703	12.5%	9.8%	2.4%
	Vertical	0.62	0.62	0.7	12.9%	12.9%	0.0%
	Smooth	0.625	0.635	0.703	12.5%	10.7%	1.6%
Cylinder	Diamond	0.54	0.565	0.69	27.8%	22.1%	4.6%
	Inclined	0.555	0.595	0.695	25.2%	16.8%	7.2%
	Horizontal	0.625	0.64	0.715	14.4%	11.7%	2.4%
	Vertical	0.57	0.575	0.705	23.7%	22.6%	0.9%
	Smooth	0.637	0.635	0.7	9.9%	10.2%	-0.3%
Barrel	Diamond	0.53	0.55	0.68	28.3%	23.6%	3.8%
	Inclined	0.54	0.57	0.65	20.4%	14.0%	5.6%
	Horizontal	0.56	0.57	0.68	21.4%	19.3%	1.8%
	Vertical	0.625	0.63	0.62	-0.8%	-1.6%	0.8%
	Smooth	0.62	0.635	0.7	12.9%	10.2%	2.4%
Hyperboloidal	Diamond	0.435	0.49	0.695	59.8%	41.8%	12.6%
	Inclined	0.575	0.565	0.705	22.6%	24.8%	-1.7%
	Horizontal	0.625	0.63	0.71	13.6%	12.7%	0.8%
	Vertical	0.585	0.6	0.67	14.5%	11.7%	2.6%
	Smooth	0.625	0.635	0.7	12.0%	10.2%	1.6%

- For the Al-Al pair of materials we observe that:

● the biggest differences in time are registered for the diamond geometry of the gripping area (with differences up to 43%);
● for the other geometries of the gripping area, the differences are smaller but still significant;
● for the parallelepiped-shaped Objects, the differences in time are small regardless of the gripping regions geometry;
● these differences are more pronounced for the other cases;
● for the smooth geometry of the gripping area, these differences are very small;
● as expected, the barrel-shaped Object is the most difficult to keep in a still position (with an exception for the diamond and vertical geometry of the gripping area. In this case, it seems that this geometry allows a better contact area between the Object and the gripper).

- For the Al-Necuron pair of materials we observe that:

● for the diamond geometry of the gripping area, the trend encountered in the case of Al-Al pair of materials is also visible, although with smaller amplitude;

- in the case of the smooth gripping geometry, there is no difference between the four Object geometries;
- we can appreciate that the pairs Al-Al and Al-Necuron behave quite similarly;
- as expected, again, the barrel-shaped Object is the most difficult to keep in a still position (with an exception for the diamond and vertical geometry of the gripping area). In this case, it seems that this geometry allows a larger contact area between the Object and the gripper - this confirms the results for Al-Al pair of materials.

- For the Necuron-Necuron pair of materials we observe that:

- for the diamond geometry of the gripping area, in this case, there are almost no significant differences between the four Object geometries;
- again, for the smooth gripping geometry there is no difference between the four Object geometries;
- in general, with a small exception for the vertical geometry of the gripping area, the values for the moments in time when the Object starts to move are smaller;
- the barrel-shaped object is again the most difficult case, this time with no exception.

As general conclusions on what geometry is better for different types of Objects, we can formulate the following statements:

- For the parallelipiped Object:

- for all pairs of materials, there are few differences between the five geometries of the gripping region;
- the Necuron-Necuron pair of materials provides the best performances.

- For the cylindrical Object:

- for the Al-Al and Al-Necuron pairs of materials, horizontal and smooth geometries provide the best results;
- for the Necuron-Necuron pair of materials, horizontal geometry provides the best results.

- For the barrel-shaped object:

- for all pairs of materials, horizontal and smooth geometries provide the best results.

- For the hyperboloidal Object:

- for the Al-Al and Al-Necuron pairs of materials, horizontal and smooth geometries provide the best results;
- for Necuron-Necuron, there are small differences between the five geometries.

Finally, we make the observation that for the hyperboloidal Object, due to the shape, the contact region induces numerical instabilities in the FEA approach.

References

[1]. Dharbaneshwer S. J., Subramanian S. J., Kohlhoff K., *Robotic grasp analysis using deformable solid mechanics*, Meccanica, vol. 54, p. 1767-1784, 2019.

[2]. Turrell Y. N., Li F.-X., Wing A. M., *Estimating the minimum grip force required when grasping objects under impulsive loading conditions*, Behavior Research Methods, Instruments, & Computers, vol. 33(1), p. 38-45, 2001.

[3]. Sathishkumar A., *et al.*, *Design and Analysis of a Multi Fingered Gripper for Grasping Irregular Objects*, International Research Journal of Engineering and Technology (IRJET), vol. 04(3), 2017.

[4]. Hao Y., *et al.*, *Modeling and experiments of a soft robotic gripper in amphibious environments*, International Journal of Advanced Robotic Systems, May-June, p. 1-12, DOI: 10.1177/1729881417707148, 2017.

[5]. Miller A. T., Allen P. K., *Examples of 3D Grasp Quality Computations*, Proceedings of the IEEE International Conference on Robotics & Automation, Detroit, Michigan, May 1999.

[6]. Lu Q., *et al.*, *An Origami-Inspired Variable Friction Surface for Increasing the Dexterity of Robotic Grippers*, IEEE Robotics and Automation Letters, vol. 5(2), p.2538-2545, DOI: 10.1109/LRA.2020.2972833, 2020.

[7]. Sahbani A., El-Khoury S., Bidaud P., *An overview of 3D object grasp synthesis algorithms*, Robotics and Autonomous Systems, vol. 60 (3), p. 326-336, 2012.

[8]. Ferrari C., Canny J., *Planning Optimal Grasp*, Proceedings IEEE International Conference on Robotics and Automation, DOI: 10.1109/ROBOT.1992.219918, May 1992.

[9]. Romeo R. A., *et al.*, *Slippage Detection with Piezoresistive Tactile Sensors*, Sensors, vol. 17(8), p. 1844, DOI: 10.3390/s17081844, 2017.

[10]. Hu Al., Peachey B., *Redesigning an Experiment to Determine the Coefficient of Friction*, Journal of Emerging Investigators, June 2016.

[11]. Kapucu S., *A simple experiment to measure the maximum coefficient of static friction with a smartphone*, Phys. Educ. 53, 053006 (3pp), 2018.

[12]. Dickey R. D. I., Jackson R. L., Flowers G. T., *Measurements of the Static Friction Coefficient Between Tin Surfaces and Comparison to a Theoretical Model*, Journal of Tribology, vol. 133 (3), DOI: 10.1115/1.4004338, 2011.

[13]. Lee C-H., Polycarpou A. A., *Static Friction Experiments and Verification of an Improved Elastic-Plastic Model Including Roughness Effects*, Journal of Tribology, vol. 129(4), DOI: 10.1115/1.2768074, 2007.

[14]. Metcalfe A., *et al.*, *Statistics in Engineering: With Examples in MATLAB® and R*, Second Edition, Chapman and Hall/CRC, New York, 2019.

[15]. Groß T., *Technische Produktdokumentation: Detaillierungsfunktionen mit Siemens NX*, 978-3-658-28266-0, Springer Fachmedien Wiesbaden, Springer Vieweg, 2020.

[16]. Tickoo S., *Siemens NX 12.0 for Designers*, 11th Edition, 1640570128, 9781640570122, CADCIM Technologies, 2018.

[17]. ***, *ANSYS Inc. Theory Reference*, Canonsburg: SAS IP Inc.